ACS chemical biology

LETTERS

pubs.acs.org/acschemicalbiology

A Brain-Permeable Small Molecule Reduces Neuronal Cholesterol by Inhibiting Activity of Sirtuin 2 Deacetylase

David M. Taylor,[†] Uma Balabadra,[‡] Zhongmin Xiang,[⊥] Ben Woodman,[§] Sarah Meade,[⊥] Allison Amore,[⊥] Michele M. Maxwell,[⊥,¶] Steven Reeves,[⊥] Gillian P. Bates,[§] Ruth Luthi-Carter,[†] Philip A. S. Lowden,[‡] and Aleksey G. Kazantsev[⊥,¶,*]

[†]Brain Mind Institute, Ecole Polytechnique Fédérale de Lausanne, 1015 Lausanne, Switzerland

[‡]Department of Biological Sciences, Birkbeck, University of London, Malet Street, London WC1E 7HX, U.K.

[§]Department of Medical and Molecular Genetics, King's College London, Eighth Floor Tower Wing, Guy's Hospital, Great Maze Pond, London SE1 9RT, U.K.

[⊥]MassGeneral Institute for Neurodegenerative Disease, Massachusetts General Hospital, Charlestown, Massachusetts 02129, United States

[¶]Harvard Medical School, Boston, Massachusetts 02129, United States

ABSTRACT: Sirtuin 2 (SIRT2) deacetylase-dependent inhibition mediates neuroprotective reduction of cholesterol biosynthesis in an *in vitro* Huntington's disease model. This study sought to identify the first brain-permeable SIRT2 inhibitor and to characterize its cholesterol-reducing properties in neuronal models. Using biochemical sirtuin deacetylation assays, we screened a brain-permeable *in silico* compound library, yielding 3-(1-azepanylsulfonyl)-*N*-(3-bromphenyl)benzamide as the most potent and selective SIRT2 inhibitor. Pharmacokinetic studies demonstrated brain-permeability but limited metabolic stability of the selected candidate. In accordance with previous observations, this SIRT2 inhibitor stimulated cytoplasmic retention of sterol regulatory element binding protein-2 and subsequent transcriptional downregulation of cholesterol biosynthesis genes, resulting in reduced total cholesterol in primary striatal neurons. Furthermore, the identified inhibitor reduced cholesterol in cultured naïve neuronal cells and brain slices from wild-type mice. The outcome of this study provides a clear opportunity for lead optimization and drug development, targeting metabolic dysfunctions in CNS disorders where abnormal cholesterol homeostasis is implicated.

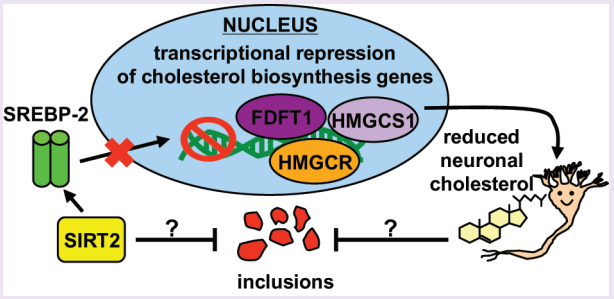

Sirtuin 2 (SIRT2) is one of seven human sirtuins (SIRT1–SIRT7) comprising the class III histone deacetylase (HDAC) family, which are unique for their NAD-dependent catalytic activities.[1] Known SIRT2 substrates include α-tubulin,[2] FOXO1, FOXO3a, p53 and histones 3 and 4,[1] and likely others as yet unidentified. In dividing cells, SIRT2 regulates mitosis and cytoskeleton dynamics, while its function(s) in terminally differentiated neurons are just beginning to be elucidated.[2−5]

A role for sirtuins as therapeutic targets in age-dependent neurodegenerative disorders has recently emerged, primarily due to their functions as regulators of metabolism and subsequent effects on longevity.[1] To that end, most of these studies have focused on the neuroprotective effects of SIRT1 activation.[6] We previously reported on inhibition of SIRT2 activity as a neuroprotective modality in Parkinson's and Huntington's disease (HD) models.[7,8] In the latter study, genetic or pharmacologic inhibition of SIRT2 in a striatal neuron model of HD[8] resulted in significant downregulation of RNAs encoding enzymes responsible for sterol biosynthesis, which subsequently led to a reduction in total cholesterol levels.[8] Whereas exposure to mutant huntingtin protein increased sterol levels in primary neurons, SIRT2 inhibition reduced this accumulation, apparently by decreasing nuclear trafficking of the sterol regulatory element binding protein-2 (SREBP-2) transcription factor.

According to a recent report, brain cholesterol levels are reduced during progression of HD,[9] which could be a compensatory effect, suggesting greater benefits from early intervention with SIRT2-based therapeutics. However, while our studies have focused mostly on a new regulatory role of SIRT2 in HD models,[8] this novel pathway could have a broader application in other neurological conditions, such as Alzheimer's disease, for which modulation of cholesterol and other associated metabolic pathways might be of therapeutic benefit.

RESULTS AND DISCUSSION

Target validation in murine disease models is an essential step prior to expensive and tedious drug development. Genetic

Received: November 17, 2010
Accepted: March 3, 2011
Published: March 03, 2011

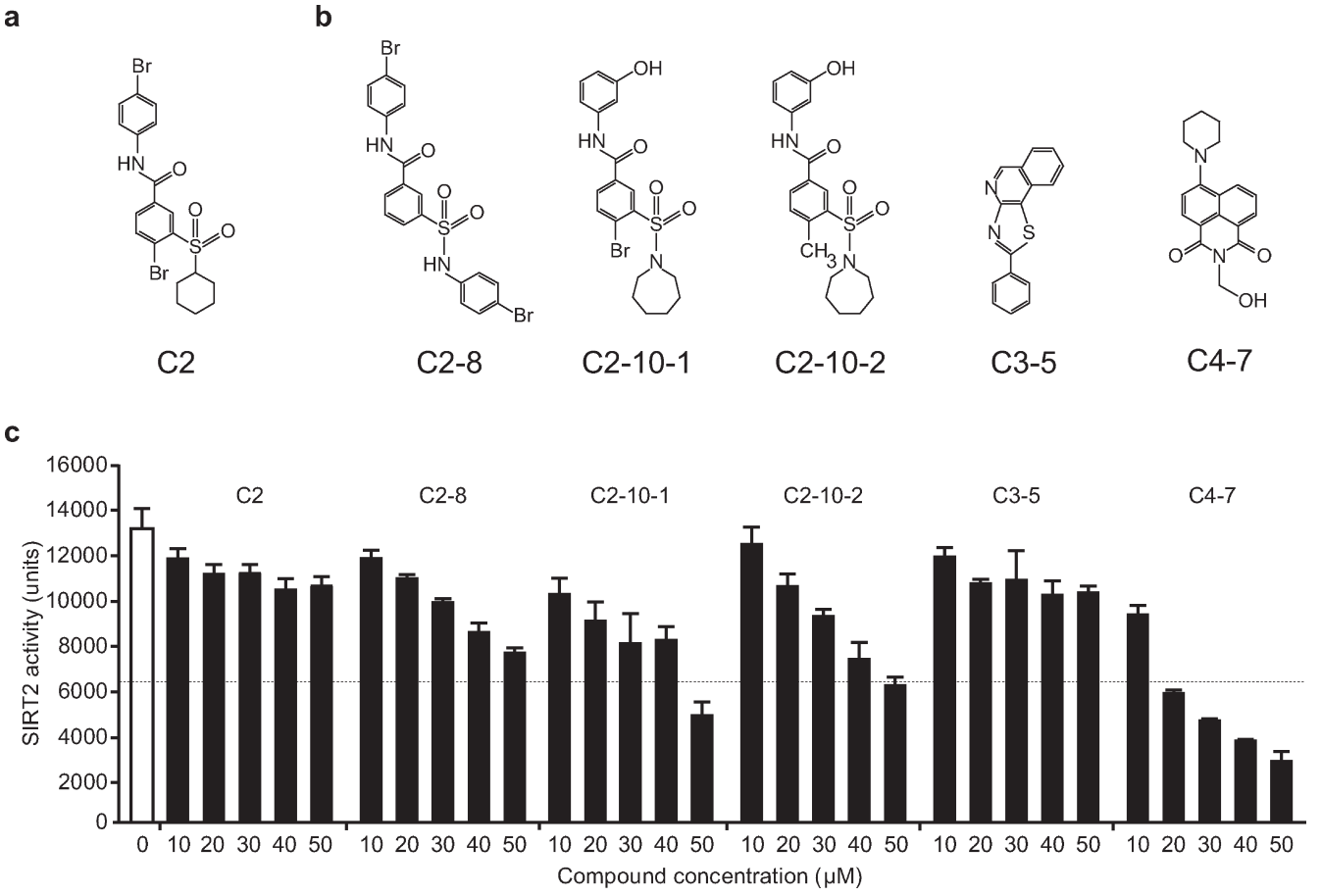

Figure 1. SIRT2 activities of previously identified aggregation inhibitors. (a) Structure of sulfobenzoic acid derivative C2, identified as the primary hit in a yeast polyglutamine toxicity screen. (b) Structures of compounds optimized in a mammalian aggregation model; C2 structural analogues C2-8, C2-10-1, C2-10-2, and structurally diverse C3-5 and C4-7. (c) Compound dose−response tests using an *in vitro* deacetylase assay. Each compound dose was tested in triplicate. Dashed line represents 50% of control SIRT2 activity (white bar).

validation often relies on generation of knockout mice or RNAi-driven knockdown of the target protein. Both genetic manipulations can produce uncontrollable compensatory effects, obscuring interpretation. Further, both methods remove the modality of interest from native protein complexes, which can cause unpredictable effects, and poorly mimic transient interactions of small molecules with the target. Thus, we reasoned that pharmacological target validation with small molecular probes is more conclusive and consistent with the goal of drug development. Previously identified SIRT2 inhibitors lack brain-permeable properties,[7] preventing animal efficacy studies, and thus in this work we sought to identify such brain-permeable compounds and their respective structural scaffold(s).

Sulfobenzoic Acid Derivatives as SIRT2 Inhibitors. Previous work has demonstrated a relationship between SIRT2 activity and aggregation that remains enigmatic.[7,8] However, an effect on SIRT2 is conceivably intrinsic to the effects of some aggregation inhibitors and useful for identification of bioactive compounds and respective structural scaffolds. On that premise, we examined compounds previously optimized for polyglutamine aggregate inhibition in mammalian cell-based assays[10] for an effect on SIRT2 deacetylase activity. The panel, consisting of aggregation inhibitors derived from three structural scaffolds (C2, C3, C4), was tested with a biochemical SIRT2 deacetylation assay (Figure 1).[7,11] Sulfobenzoic acid derivative C2, the primary hit in a yeast polyglutamine toxicity screen and a modest aggregation inhibitor in mammalian cells, did not show dose-dependent SIRT2 inhibition (Figure 1, panels a and c).[10] In contrast, its structural analogues, including C2-8,[10] C2-10-1, and C2-10-2, identified in a second screen of a C2 focused library (Figure 1, panel b) as optimal polyglutamine aggregation inhibitors, demonstrated dose-dependent SIRT2 inhibition (Figure 1, panel c). A structurally diverse aggregation inhibitor, C4-7,[10] also showed SIRT2 inhibition activity, while the benzothiazol derivative C3-5 [10] did not (Figure 1, panels b and c). The C4 scaffold was not pursued due to anticipated cytotoxic properties of its analogues.

Notably, in this and previous studies, we observed consistent association between identified bioactive sulfobenzoic acid derivatives and SIRT2 inhibition activity.[7,8,10] Furthermore, excellent drug-like properties and brain permeability have been demonstrated by the sulfobenzoic acid derivative C2-8, a previously described neuroprotective polyglutamine aggregation inhibitor.[12] Though it is unclear whether C2-8 or its metabolite act as SIRT2 inhibitor(s) *in vivo*, excellent pharmacological properties of sulfobenzoic acid derivative(s) suggest utility of the scaffold for CNS drug development. Thus, we selected the structural scaffold of sulfobenzoic acid derivatives for development of potent and selective brain-permeable SIRT2 inhibitors.

Sulfobenzoic Acid Derivative AK-7 Is an *in Silico* SIRT2 Inhibitor. To reach that objective, we performed a substructural search (Figure 2, panel a) of a diverse library of 389,813

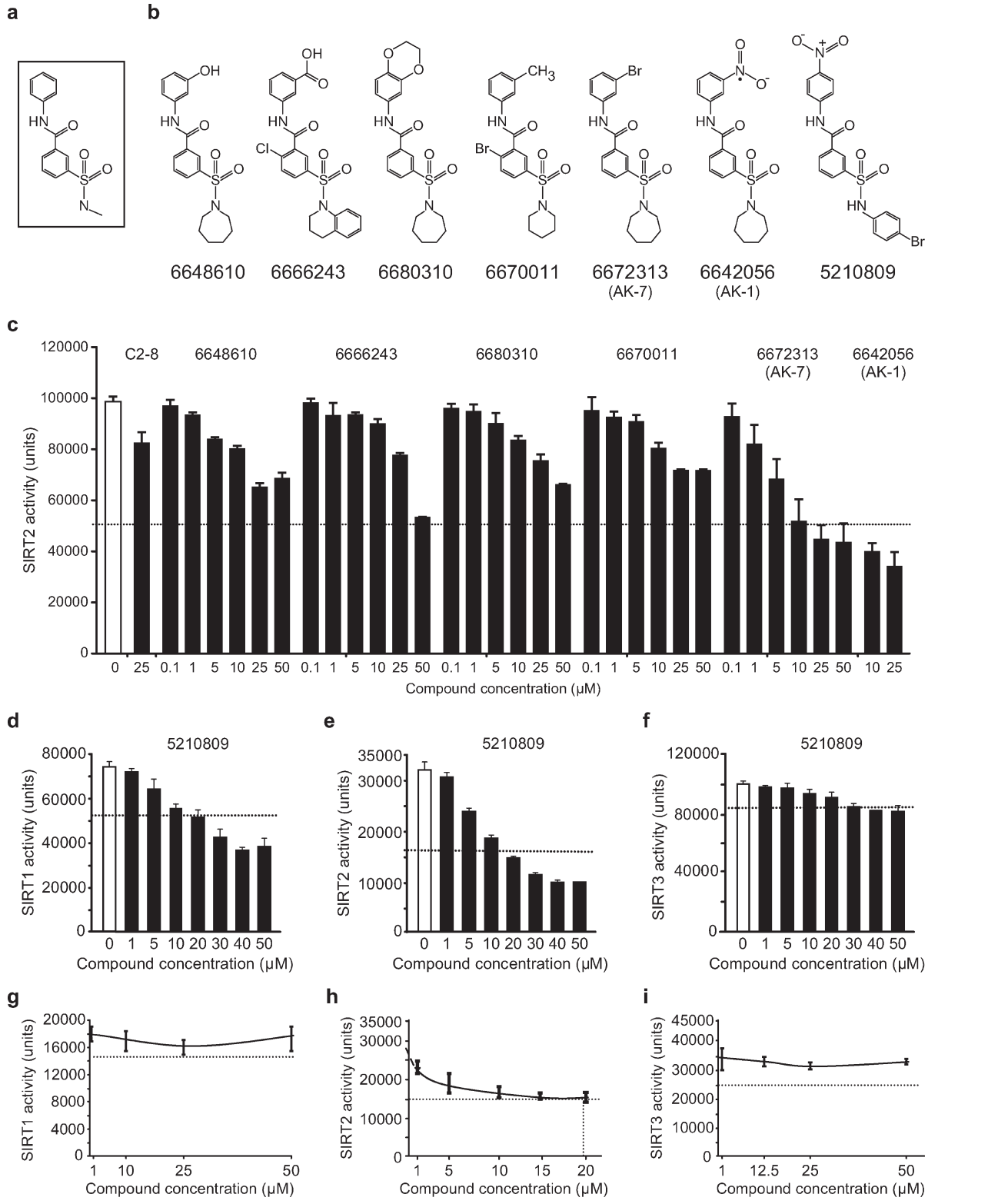

Figure 2. Identification of a brain-permeable SIRT2 inhibitor, the sulfobenzoic acid derivative AK-7. (a) Substructure used to design an *in silico* focused library of brain-permeable sulfobenzoic acid derivatives. (b) Representative structures of brain-permeable sulfobenzoic acid derivatives from the *in silico* library and AK-1. (c–i) Activity tests on representative sulfobenzoic acid derivatives using *in vitro* sirtuin deacetylase assays with recombinant (c, e, h) SIRT2, (d, g) SIRT1, and (f, i) SIRT3. Each compound dose was tested in triplicate. (d–i) Dose–response tests to establish compound selective inhibition of SIRT2 activity. (g–i) Compound 6672313 (AK-7) shows highly selective inhibition of SIRT2 (IC_{50} = 15.5 μM). Dashed lines represent 50% (c, e, h), 25% (d, g), and 25% (f, i) of control SIRT2, SIRT1, and SIRT3 activities (white bars), respectively.

dx.doi.org/10.1021/cb100376q |*ACS Chem. Biol.* 2011, 6, 540–546

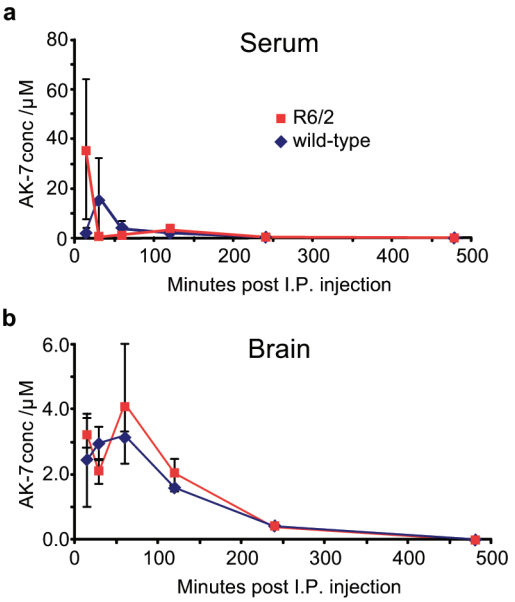

Figure 3. Pharmacokinetics of AK-7 in wild-type and HD mice. (a) AK-7 time course in serum of wild-type (blue diamonds) and transgenic R6/2 HD mice (red squares). AK-7 was rapidly eliminated from serum, with peak serum concentrations occurring between 15 and 30 min post administration. (b) AK-7 time course in brain of wild-type (blue diamonds) and transgenic R6/2 HD mice (red squares). Peak brain concentrations for AK-7 were 3 μM in wild-type and 4 μM in R6/2 mice, decreasing to 0.2 μM after 4 h.

compounds (ChemBridge) and identified 1,257 sulfobenzoic acid derivatives; 223 of these were identified in a CNS sublibrary of 50,047 compounds with *in silico*-predicted brain permeability. A small fraction of these are shown in Figure 2, panel b. Analogs were then tested in dose−response experiments using biochemical SIRT2 deacetylation assays (Figure 2, panel c).[7] Compounds demonstrating at least 50% inhibition of SIRT2 activity in the tested concentration range (0.1−50 μM) were prioritized and retested in SIRT1, 2, and 3 deacetylation assays to determine selectivity (Figure 2, panels d−f). Those demonstrating equal or greater than 25% inhibition of SIRT1 or SIRT3 (Figure 2, panels d−f) were eliminated to ensure high SIRT2 specificity.

The analysis yielded only one candidate compound, 3-(1-azepanylsulfonyl)-*N*-(3-bromphenyl)benzamide, that satisfied the above criteria (Figure 2, panels b, c, g−i). The compound, named AK-7, demonstrated selective inhibition of SIRT2 *in vitro* (IC_{50} = 15.5 μM) and is a close structural analogue of 3-(1-azepanylsulfonyl)-*N*-(3-nitrophenyl)benzamide (AK-1, SIRT2 IC_{50} = 12.5 μM), an efficacious inhibitor in neurodegenerative disease models.[7,8]

AK-7 Is Brain-Permeable. To assess pharmacokinetics, AK-7 (1.5 mg/mL^{-1} in 25% Cremophor/10% DMSO in water) was administered by intraperitoneal injection to wild-type and R6/2 HD model mice[13] at 15 mg/kg/dose. Brain and serum samples were collected after 15, 30, 60, 120, 240, and 480 min (n = 3/genotype/time point). AK-7 was rapidly eliminated from serum with a peak concentration before 30 min post injection and negligible levels detected after 1 h (Figure 3, panel a). Brain permeability was observed with peak concentrations of 3−4 μM, but only 2 μM remained 2 h post injection (Figure 3, panel b), which suggested that achieving metabolic stability in the brain may require further optimization of the lead by chemical modifications. However, it remains promising that the kinetics of brain penetration was similar in wild-type and R6/2 mice, suggesting that HD-related phenotypes do not compromise (nor enhance) the compound's brain penetration.

AK-7 Is Efficacious in an *in Vitro* Neuronal HD Model. Treatment with AK-7 resulted in protection of neurons in an *in vitro* model of HD (Figure 4, panel a), and the number of inclusions per neuron was also reduced (Figure 4, panel b). Neither of these effects is attributable to a change in expression of mutant huntingtin due to AK-7 treatment, as assessed by Western blot (Figure 4, panel c). The achieved concentration of the compound in brain (however transient) corresponded to the observed neuroprotective dose (1 μM), despite being below its IC_{50} (Figure 2, panel h). That result encourages testing metabolically stable structural analogue(s) of AK-7 in HD mouse models.

AK-7 Is a Cholesterol Reducer in Neuronal Models. To verify the cholesterol-reducing properties of AK-7 in neuronal models, it was compared to the biological outcomes previously described for AK-1,[8] for which it has a similar ability to inhibit SIRT2 activity *in vitro* (Figure 4, panel d). In concordance with our previous results,[8] SIRT2-dependent nucleo-cytoplasmic trafficking of the master regulator of cholesterol biosynthesis, SREBP-2, was reduced by AK-7 in primary striatal neurons (Figure 4, panels e and f). Subsequent transcriptional downregulation of cholesterol biosynthetic genes was highly significant (Figure 4, panel g) and resulted in AK-7-dependent reduction of total cholesterol levels (Figure 4, panel h). We then extended the experiments to naïve N2a neuroblastoma cells and hippocampal slice cultures from wild-type mice. In both models, AK-7 reduced cholesterol levels at 10 μM, but was ineffective at a lower concentration (Figure 4, panels i and j). The more potent *in vitro* SIRT2 inhibitor AK-1, reduced cholesterol at a lower dose in both models (Figure 4, panels i and j).

This study identified the sulfobenzoic acid derivative AK-7 as a brain-permeable SIRT2 inhibitor that is capable of reducing neuronal cholesterol levels. Although only a low micromolar concentration was achieved in the brain under the tested conditions (1 order of magnitude below its *in vitro* IC_{50}), the results established an important proof of principle. However, it is imperative to optimize this lead for potency and metabolic stability by chemical modifications. The identified scaffold of sulfobenzoic acid derivatives clearly presents such an opportunity for medicinal chemistry, since design and organic synthesis of diverse structural analogues can be accomplished in a few simple steps.

The cholesterol-reducing properties of AK-7 were highly consistent with the previously established effects of SIRT2 inhibition.[8] These include cytoplasmic retention of SREBP-2, transcriptional downregulation of genes responsible for sterol biosynthesis, and subsequent cholesterol reduction in three neuronal models at a concentration (10 μM) consistent with its *in vitro* SIRT2 inhibition activity (IC_{50} = 15.5 μM). In contrast, the neuroprotective effect of AK-7 in an HD model was achieved at a low dose (1 μM), which is encouraging for the sake of HD drug development, though it might indicate off-target effects. Alternatively, SIRT2 inhibition might independently modulate several neuroprotective pathways, such as cholesterol biosynthesis and aggregation, allowing cumulative beneficial effects to be achieved at lower concentrations.

The discovery of the first brain-permeable SIRT2 inhibitor and its respective scaffold create a foundation for further optimization to achieve increased potency and stability, en route

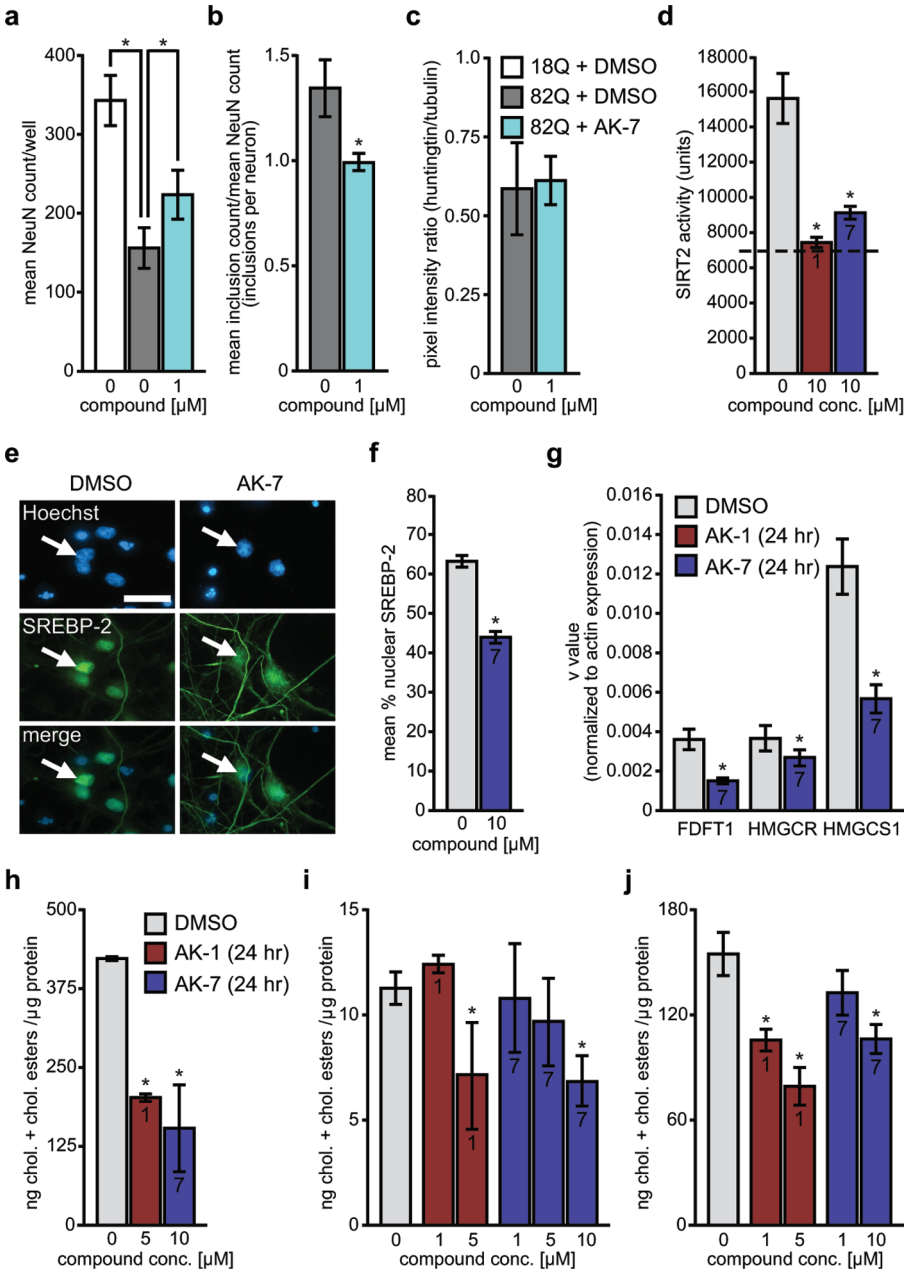

Figure 4. Bioactivity of AK-7 in *in vitro* neuronal models. (a) Neuroprotective effect of AK-7 in striatal HD neurons. Lentivirally transduced expression of mutant huntingtin fragment N171-82Q (gray bar), but not wild-type fragment N171-18Q (white bar), led to significant neuronal cell death, rescued by AK-7 (blue bar). (b) AK-7 decreases the number of polyglutamine inclusions in HD neurons. (c) AK-7 does not alter huntingtin transgene expression. (d) *In vitro* SIRT2 inhibitory activities of structural analogues AK-1 (red bar) and brain-permeable AK-7 (blue bar) at 10 μM. (e, f) AK-7 decreases the nuclear localization of SREBP-2. (e) Representative images of reduced SREBP-2 nuclear localization following AK-7 treatment using Hoechst staining to delineate the neuronal nucleus. (Scale bar: 10 μm). (f) Quantification of the percentage of total endogenous SREBP-2 localized to neuronal nuclei following AK-7 treatment. (g) AK-7 decreases the levels of RNAs encoding sterol biosynthetic enzymes. (h–j) AK-1 (red bars) and AK-7 (blue bars) significantly reduce total cholesterol levels in primary striatal neuron cultures (h), N2a cells (i). and hippocampal brain slices (j). For compound treated samples, bars are labeled as 1 for AK-1 and 7 for AK-7.

to preclinical efficacy testing in Huntington's and Parkinson's disease mouse models. In addition, optimized SIRT2 inhibitors may provide critical pharmacological reagents to target metabolic dysfunctions in various human illnesses where cholesterol homeostasis is implicated. These include common neurodegenerative diseases (notably Alzheimer's disease), rare cholesteryl ester storage disorders, and extremely prevalent metabolic and cardiovascular conditions.[14−16]

METHODS

Compound Source and Storage. Compounds were procured from Chembridge, dissolved in molecular biology grade dimethyl sulfoxide (DMSO) to 10 mM, and stored as aliquots at −80 °C.

Sirtuin Biochemical Deacetylation Assays. Sirtuin activity was assessed using the Fleur de Lys assay (BioMol International, LP) with recombinant active enzymes SIRT1 (BioMol-SE-239), SIRT2 (BioMol-SE-251),

and the catalytically active fragment of SIRT3 (BioMol-SE-251), as described previously.[7,11] Results were measured using a Perkin-Elmer Victor^{2}V 1420 Multilabel plate reader (excitation 355 nm, emission 460 nm).

Assays were performed using the manufacturer's recommendations, and each compound concentration was tested in triplicate. For each experiment, SIRT1 activity was normalized to 1 U/reaction well and SIRT2 and SIRT3 activity to 5 U/reaction well (where U = 1 pmol/min at 37 °C, 250 μM substrate, 500 μM NAD^+). Each reaction well contained enzyme, 500 μM NAD^+ (BioMol-KI-282), 250 μM fluorogenic deacetylase substrate (BioMol-KI-177), supplied reaction buffer, and the compound of interest or mock control (DMSO) in a total volume of 50 μL. Autofluorescent backgrounds were measured in triplicate in reaction solutions containing substrate, buffer, and NAD^+ in triplicate and subtracted from experimental signals.

Formulation and Detection of AK-7 in Mouse Brain. AK-7 (Chembridge), solubilized at 1.5 mg/mL in 25% Cremophor EL (BASF)/ 10% DMSO in water, was administered by intraperitoneal injection to 11 week old mice at 15 mg/kg/dose, and compound levels in serum and brain were measured following sacrifice. Experiments with live animals were performed according to U.K. regulations. Blood was collected and centrifuged at 7,000 rpm for 7 min, and then serum was aspirated and immediately frozen in liquid nitrogen. Brains were immediately frozen in liquid nitrogen and stored at −80 °C. Brains were weighed and then homogenized in four volumes of 10% Cremophor RH40 in water using a Polytron homogenizer, and 2% v/v phosphoric acid was added to the homogenate, vortexed, and centrifuged at 10,000*g* at 25 °C for 1 h. The supernatant was aspirated, and solid phase extraction was performed immediately. Serum samples were vortexed into 2% v/v phosphoric acid and centrifuged at 2500 rpm for 10 min.

Samples (total collected serum or 1 mL homogenate supernatant) were then spiked with an internal standard of *N*-(4-bromo-phenyl)-3-(4-bromo-phenylsulfamoyl)-benzamide/DMSO to 5 μM and passed through 1 mL Oasis HLB SPE cartridges (Waters), preconditioned with 1 mL of methanol followed by 1 mL of water. The adsorbent was washed with three volumes of 5% methanol in water, and the sample was eluted with 0.5 mL of methanol and stored at −80 °C until HPLC.

HPLC Analysis. Samples were analyzed by HPLC on an Agilent 1100 system. Twenty microliters of each sample was injected onto a Zorbax C8 5 μm column (4.6 × 150 mm) and eluted with 67:33 acetonitrile/water at 0.7 mL/min at 20 °C, with UV absorption at 270 nm. For brain and serum, the calibration curve was prepared with 1, 5, 10, 25, and 50 μM samples. Good linearity was observed for both (R-squared: serum = 0.9603, brain = 0.9937). Blank samples provided a clean baseline for AK-7 internal standard.

Primary Neuronal Cultures. Neuronal nuclear antigen (NeuN)-positive neurons and some astroglia were derived from mechanically dissociated ganglionic eminences of E16 rat embryos. The HD model based on the expression of mutant huntingtin has been described previously.[8] Treatments of cultures with AK-7 were at 10 μM for 24 h unless stated otherwise.[8] DMSO was included at the same concentrations as a control. Lower dose, chronic treatments with AK-7 were introduced to neurons at DIV4 and continued weekly coinciding with normal medium change.

Immunocytochemistry and Western Blotting. Immunolabeling and Western blotting was performed as previously described.[8] Images for quantitative analysis were acquired with a BD Pathway 855 Bioimager (BD Biosciences) and analyzed with NIH Image J software.

Evaluation of SREBP-2 Compartmentalization. Primary neurons on coverslips were labeled for endogenous SREBP-2 and images were obtained from 30 random fields using a Leica DMI 4000 microscope (40X). Images were independently blinded prior to analysis. Nuclei were traced using Image J, and pixel density was measured as a percentage value of the soma. The number of neurons evaluated varied for each condition (DMSO n = 202, AK-7 n = 161).

Gene Expression Analysis. RNA was extracted using the RNeasy system (Qiagen AD) following the manufacturer's protocol, ethanol precipitated, and reverse transcribed with the High Capacity cDNA Reverse Transcription Kit (Applied Biosystems). Analysis of samples used the Applied Biosystems 7900HT Real-Time PCR System and SDS 2.3 software, with a cDNA input of 2 ng/test.

Inclusion Analysis. Quantification of inclusion total was performed as previously described.[8] Inclusions were labeled with antihuntingtin antibody and imaged with a BD Pathway 855 Bioimager. Image J was used for analysis.

Cholesterol Assay. Total sterols were measured in primary cultures using the Amplex Red Cholesterol Assay Kit (Invitrogen Molecular Probes), with modifications as described in ref 8.

Hippocampal Slice Culture. Hippocampal slice cultures were established as previously described[17] and treated with DMSO or AK-7 (1 or 10 μM) for 48 h. After PBS rinsing, slices were removed from inserts and sonicated in PBS. Protein content was measured using a Bradford assay (BioRad). Total cholesterol and cholesterol ester levels were measured using an enzymatic assay kit (Cayman) following the manufacturer's instructions and expressed as ng/μg protein.

N2a Cell Culture. N2a neuroblastoma cells, maintained in culture as described previously,[18] were treated with DMSO or AK-7 at indicated concentrations for 48 h, and cholesterol was assessed as described above for brain slices.

Statistical Analysis. For pairwise samples in bioactivity experiments, one-tailed Student's t tests were used to analyze significance following assessment of normality and equal variance. Significance was attributed to P values below 0.05 and is represented by an asterisk.

AUTHOR INFORMATION

Corresponding Author
*E-mail: akazantsev@partners.org.

ACKNOWLEDGMENT

We thank M. Forrest and L. Feletti for help with culture preparation. This work was supported by the Carmen Foundation, the RJG Foundation, the Michael J. Fox Foundation for Parkinson's Research, the CHDI Foundation, the Ecole Polytechnique Fédérale de Lausanne, and the Swiss National Science Foundation.

REFERENCES

(1) Taylor, D. M., Maxwell, M. M., Luthi-Carter, R., and Kazantsev, A. G. (2008) Biological and potential therapeutic roles of sirtuin deacetylases. *Cell. Mol. Life Sci. 65*, 4000–4018.

(2) North, B. J., Marshall, B. L., Borra, M. T., Denu, J. M., and Verdin, E. (2003) The human Sir2 ortholog, SIRT2, is an NAD+-dependent tubulin deacetylase. *Mol. Cell 11*, 437–444.

(3) North, B. J., and Verdin, E. (2007) Mitotic regulation of SIRT2 by cyclin-dependent kinase 1-dependent phosphorylation. *J. Biol. Chem. 282*, 19546–19555.

(4) Pandithage, R., Lilischkis, R., Harting, K., Wolf, A., Jedamzik, B., Luscher-Firzlaff, J., Vervoorts, J., Lasonder, E., Kremmer, E., Knoll, B., and Luscher, B. (2008) The regulation of SIRT2 function by cyclin-dependent kinases affects cell motility. *J. Cell Biol. 180*, 915–929.

(5) Renthal, W., Kumar, A., Xiao, G., Wilkinson, M., Covington, H. E., Maze, I., Sikder, D., Robison, A. J., LaPlant, Q., Dietz, D. M., Russo, S. J., Vialou, V., Chakravarty, S., Kodadek, T. J., Stack, A., Kabbaj, M., and Nestler, E. J. (2009) Genome-wide analysis of chromatin regulation by cocaine reveals a role for sirtuins. *Neuron 62*, 335–348.

(6) Parker, J. A., Arango, M., Abderrahmane, S., Lambert, E., Tourette, C., Catoire, H., and Neri, C. (2005) Resveratrol rescues mutant polyglutamine cytotoxicity in nematode and mammalian neurons. *Nat. Genet. 37*, 349–350.

(7) Outeiro, T. F., Kontopoulos, E., Altmann, S. M., Kufareva, I., Strathearn, K. E., Amore, A. M., Volk, C. B., Maxwell, M. M., Rochet, J.-C., McLean, P. J., Young, A. B., Abagyan, R., Feany, M. B., Hyman, B. T., and Kazantsev, A. G. (2007) Sirtuin 2 inhibitors rescue alpha-synuclein-mediated toxicity in models of Parkinson's disease. *Science 317*, 516–519.

(8) Luthi-Carter, R., Taylor, D. M., Pallos, J., Lambert, E., Amore, A., Parker, A., Moffitt, H., Smith, D. L., Runne, H., Gokce, O., Kuhn, A., Xiang, Z., Maxwell, M. M., Reeves, S. A., Bates, G. P., Neri, C., Thompson, L. M., Marsh, J. L., and Kazantsev, A. G. (2010) SIRT2 inhibition achieves neuroprotection by decreasing sterol biosynthesis. *Proc. Natl. Acad. Sci. U.S.A. 107*, 7927–7932.

(9) Valenza, M., Leoni, V., Karasinska, J. M., Petricca, L., Fan, J., Carroll, J., Pouladi, M. A., Fossale, E., Nguyen, H. P., Riess, O., MacDonald, M., Wellington, C., DiDonato, S., Hayden, M., and Cattaneo, E. (2010) Cholesterol defect is marked across multiple rodent models of Huntington's disease and is manifest in astrocytes. *J. Neurosci. 30*, 10844–10850.

(10) Zhang, X., Smith, D. L., Meriin, A. B., Engemann, S., Russel, D. E., Roark, M., Washington, S. L., Maxwell, M. M., Marsh, J. L., Thompson, L. M., Wanker, E. E., Young, A. B., Housman, D. E., Bates, G. P., Sherman, M. Y., and Kazantsev, A. G. (2005) A potent small molecule inhibits polyglutamine aggregation in Huntington's disease neurons and suppresses neurodegeneration in vivo. *Proc. Natl. Acad. Sci. U.S.A. 102*, 892–897.

(11) Mai, A., Valente, S., Meade, S., Carafa, V., Tardugno, M., Nebbioso, A., Galmozzi, A., Mitro, N., De Fabiani, E., Altucci, L., and Kazantsev, A. (2009) Study of 1,4-dihydropyridine structural scaffold: discovery of novel sirtuin activators and inhibitors. *J. Med. Chem. 52*, 5496–5504.

(12) Chopra, V., Fox, J. H., Lieberman, G., Dorsey, K., Matson, W., Waldmeier, P., Housman, D. E., Kazantsev, A., Young, A. B., and Hersch, S. (2007) A small-molecule therapeutic lead for Huntington's disease: preclinical pharmacology and efficacy of C2-8 in the R6/2 transgenic mouse. *Proc. Natl. Acad. Sci. U.S.A. 104*, 16685–16689.

(13) Mangiarini, L., Sathasivam, K., Seller, M., Cozens, B., Harper, A., Hetherington, C., Lawton, M., Trottier, Y., Lehrach, H., Davies, S. W., and Bates, G. P. (1996) Exon 1 of the HD gene with an expanded CAG repeat is sufficient to cause a progressive neurological phenotype in transgenic mice. *Cell 87*, 493–506.

(14) Liu, J.-P., Tang, Y., Zhou, S., Toh, B. H., McLean, C., and Li, H. (2010) Cholesterol involvement in the pathogenesis of neurodegenerative diseases. *Mol. Cell. Neurosci. 43*, 33–42.

(15) Durrington, P. (2003) Dyslipidaemia. *Lancet 362*, 717–731.

(16) Vitner, E. B., Platt, F. M., and Futerman, A. H. (2010) Common and uncommon pathogenic cascades in lysosomal storage diseases. *J. Biol. Chem. 285*, 20423–20427.

(17) Xiang, Z., Hrabetova, S., Moskowitz, S. I., Casaccia-Bonnefil, P., Young, S. R., Nimmrich, V. C., Tiedge, H., Einheber, S., Karnup, S., Bianchi, R., and Bergold, P. J. (2000) Long-term maintenance of mature hippocampal slices in vitro. *J. Neurosci. Methods 98*, 145–154.

(18) Raychaudhuri, S., Sinha, M., Mukhopadhyay, D., and Bhattacharyya, N. P. (2008) HYPK, a Huntingtin interacting protein, reduces aggregates and apoptosis induced by *N*-terminal Huntingtin with 40 glutamines in Neuro2a cells and exhibits chaperone-like activity. *Hum. Mol. Genet. 17*, 240–255.